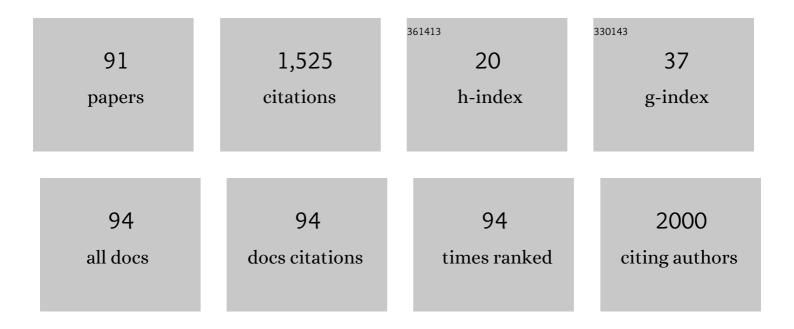
## Yuka Yamamoto

List of Publications by Year in descending order

Source: https://exaly.com/author-pdf/1912397/publications.pdf Version: 2024-02-01



#	Article	IF	CITATIONS
1	11C-methionine (MET) and 18F-fluorothymidine (FLT) PET in patients with newly diagnosed glioma. European Journal of Nuclear Medicine and Molecular Imaging, 2008, 35, 2009-2017.	6.4	148
2	Correlation of 18F-FLT and 18F-FDG uptake on PET with Ki-67 immunohistochemistry in non-small cell lung cancer. European Journal of Nuclear Medicine and Molecular Imaging, 2007, 34, 1610-1616.	6.4	144
3	Detection of Hepatocellular Carcinoma Using 11C-Choline PET: Comparison with 18F-FDG PET. Journal of Nuclear Medicine, 2008, 49, 1245-1248.	5.0	108
4	Usefulness of 3′-Deoxy-3′- <sup>18</sup> F-Fluorothymidine PET for Predicting Early Response to Chemoradiotherapy in Head and Neck Cancer. Journal of Nuclear Medicine, 2012, 53, 1521-1527.	5.0	64
5	Correlation of <sup>18</sup> F-FLT Uptake with Tumor Grade and Ki-67 Immunohistochemistry in Patients with Newly Diagnosed and Recurrent Gliomas. Journal of Nuclear Medicine, 2012, 53, 1911-1915.	5.0	64
6	Clinical usefulness of fusion of 1311 SPECT and CT images in patients with differentiated thyroid carcinoma. Journal of Nuclear Medicine, 2003, 44, 1905-10.	5.0	62
7	Correlation of FDG-PET findings with histopathology in the assessment of response to induction chemoradiotherapy in non-small cell lung cancer. European Journal of Nuclear Medicine and Molecular Imaging, 2006, 33, 140-147.	6.4	61
8	Comparative evaluation of 18F-FLT and 18F-FDG for detecting cardiac and extra-cardiac thoracic involvement in patients with newly diagnosed sarcoidosis. EJNMMI Research, 2017, 7, 69.	2.5	55
9	Head and Neck Cancer: Dedicated FDG PET/CT Protocol for Detection—Phantom and Initial Clinical Studies. Radiology, 2007, 244, 263-272.	7.3	53
10	Comparison of 18F-FLT PET and 18F-FDG PET for preoperative staging in non-small cell lung cancer. European Journal of Nuclear Medicine and Molecular Imaging, 2008, 35, 236-245.	6.4	53
11	Molecular mechanisms of [18F]fluorodeoxyglucose accumulation in liver cancer. Oncology Reports, 2014, 31, 701-706.	2.6	47
12	First-Trimester Fetal Echocardiography: Identification of Cardiac Structures for Screening from 6 to 13ÂWeeks' Gestational Age. Journal of the American Society of Echocardiography, 2017, 30, 763-772.	2.8	47
13	Hypoxia assessed by 18F-fluoromisonidazole positron emission tomography in newly diagnosed gliomas. Nuclear Medicine Communications, 2012, 33, 621-625.	1.1	42
14	Peripheral neuropathy induced by drinking water contaminated with low-dose arsenic in Myanmar. Environmental Health and Preventive Medicine, 2019, 24, 23.	3.4	38
15	Detection of colorectal cancer using 18F-FLT PET: comparison with 18F-FDG PET. Nuclear Medicine Communications, 2009, 30, 841-845.	1.1	36
16	3′-Deoxy-3′-[F-18]Fluorothymidine Positron Emission Tomography in Patients with Recurrent Glioblastoma Multiforme: Comparison with Gd-DTPA Enhanced Magnetic Resonance Imaging. Molecular Imaging and Biology, 2006, 8, 340-347.	2.6	34
17	Changes in 18F-fluorothymidine and 18F-fluorodeoxyglucose positron emission tomography imaging in patients with head and neck cancer treated with chemoradiotherapy. Annals of Nuclear Medicine, 2013, 27, 363-370.	2.2	28
18	Progression of outflow tract obstruction in the fetus. Early Human Development, 2012, 88, 279-285.	1.8	27

Үика Үамамото

#	Article	IF	CITATIONS
19	A study of the acute effect of smoking on cerebral blood flow using 99mTc-ECD SPET. European Journal of Nuclear Medicine and Molecular Imaging, 2003, 30, 612-614.	6.4	26
20	Cerebral Blood Flow and Oxygen Metabolism Measurements Using Positron Emission Tomography on the First Day after Carotid Artery Stenting. Journal of Stroke and Cerebrovascular Diseases, 2014, 23, e55-e64.	1.6	22
21	Doppler parameters of fetal lung hypoplasia and impact ofÂsildenafil. American Journal of Obstetrics and Gynecology, 2014, 211, 263.e1-263.e8.	1.3	20
22	3???-Deoxy-3???-18F-Fluorothymidine as a Proliferation Imaging Tracer for Diagnosis of Lung Tumors. Journal of Computer Assisted Tomography, 2008, 32, 432-437.	0.9	18
23	Intratumoral heterogeneity of 18F-FLT uptake predicts proliferation and survival in patients with newly diagnosed gliomas. Annals of Nuclear Medicine, 2017, 31, 46-52.	2.2	18
24	Correlation of 18F-FDG and 11C-methionine uptake on PET/CT with Ki-67 immunohistochemistry in newly diagnosed intracranial meningiomas. Annals of Nuclear Medicine, 2018, 32, 627-633.	2.2	18
25	Preliminary Results of Tc-99m ECD SPECT To Evaluate Cerebral Collateral Circulation During Balloon Test Occlusion. Clinical Nuclear Medicine, 2002, 27, 633-637.	1.3	17
26	The utility of bone scintigraphy in the assessment of mandibular metabolism during long-term bisphosphonate administration. Odontology / the Society of the Nippon Dental University, 2017, 105, 382-390.	1.9	17
27	Comparison of 4′-[methyl-11C]thiothymidine (11C-4DST) and 3′-deoxy-3′-[18F]fluorothymidine (18F-FLT PET/CT in human brain glioma imaging. EJNMMI Research, 2015, 5, 7.	) <sub>2.5</sub>	16
28	Diagnostic value of PET/CT with 11C-methionine (MET) and 18F-fluorothymidine (FLT) in newly diagnosed glioma based on the 2016 WHO classification. EJNMMI Research, 2020, 10, 44.	2.5	15
29	Disease activity and response to therapy monitored by [18F]FDG PET/CT using volume-based indices in IgG4-related disease. EJNMMI Research, 2020, 10, 153.	2.5	15
30	Correlation of 4′-[methyl-11C]-thiothymidine uptake with Ki-67 immunohistochemistry and tumor grade in patients with newly diagnosed gliomas in comparison with 11C-methionine uptake. Annals of Nuclear Medicine, 2016, 30, 89-96.	2.2	14
31	Dual-isotope SPECT using (99m)Tc-hydroxymethylene diphosphonate and (201)Tl-chloride to assess mandibular invasion by intraoral squamous cell carcinoma. Journal of Nuclear Medicine, 2002, 43, 1464-8.	5.0	14
32	Comparative evaluation of 99mTc-MIBI and 99mTc-HMDP scintimammography for the diagnosis of breast cancer and its axillary metastases. European Journal of Nuclear Medicine and Molecular Imaging, 2001, 28, 522-528.	2.1	12
33	Influence of volumetric 4′-[methyl-11C]-thiothymidine PET/CT parameters for prediction of the clinical outcome of head and neck cancer patients. Annals of Nuclear Medicine, 2017, 31, 63-70.	2.2	11
34	Association between carotid 18F-NaF and 18F-FDG uptake on PET/CT with ischemic vascular brain disease on MRI in patients with carotid artery disease. Annals of Nuclear Medicine, 2019, 33, 907-915.	2.2	11
35	European research trends in nuclear medicine. Annals of Nuclear Medicine, 2018, 32, 579-582.	2.2	10
36	An analysis of anatomical variations of the left pulmonary artery of the interlobar portion for lung resection by three-dimensional CT pulmonary angiography and thin-section images. Japanese Journal of Radiology, 2020, 38, 1158-1168.	2.4	10

Υυκα Υαμαμότο

#	Article	IF	CITATIONS
37	A Comparative Study of F-18 FDG PET and 201Tl Scintigraphy for Detection of Primary Malignant Bone and Soft-Tissue Tumors. Clinical Nuclear Medicine, 2011, 36, 290-294.	1.3	9
38	Applicability of emission-based attenuation map for rapid CBF, OEF, and CMRO2 measurements using gaseous 15O-labeled compounds. EJNMMI Physics, 2015, 2, 12.	2.7	8
39	18F-FDG PET/CT in patients with polymyositis/dermatomyositis: correlation with serum muscle enzymes. European Journal of Hybrid Imaging, 2020, 4, 14.	1.5	8
40	Unexpected Finding of Cerebral Meningioma on 11C-PiB PET. Clinical Nuclear Medicine, 2013, 38, 292-293.	1.3	7
41	Reconstruction of input functions from a dynamic PET image with sequential administration of <sup>15</sup> O <sub>2</sub> and H215O for noninvasive and ultra-rapid measurement of CBF, OEF, and CMRO <sub>2</sub> . Journal of Cerebral Blood Flow and Metabolism, 2018, 38, 780-792.	4.3	7
42	4′-[methyl-11C]-thiothymidine as a proliferation imaging tracer for detection of colorectal cancer: comparison with 18F-FDG. Annals of Nuclear Medicine, 2019, 33, 822-827.	2.2	6
43	Branch pulmonary artery Doppler parameters predict early survival–non-survival in premature rupture of membranes. Journal of Perinatology, 2020, 40, 1821-1827.	2.0	6
44	SPECT/CT imaging in 99mTc-HSA-DTPA gastrointestinal bleeding scintigraphy to localize bleeding sites. European Journal of Nuclear Medicine and Molecular Imaging, 2012, 39, 1824-1825.	6.4	5
45	Effectiveness of delayed absorbable monofilament suture in emergency cerclage. Taiwanese Journal of Obstetrics and Gynecology, 2014, 53, 382-384.	1.3	5
46	One-stop shopping 18F-FDG PET/CT in a patient with vascular type Behçet's disease. European Journal of Nuclear Medicine and Molecular Imaging, 2019, 46, 1578-1580.	6.4	4
47	Immune checkpoint inhibitor myocarditis mimicking Takotsubo cardiomyopathy on MPI. Journal of Nuclear Cardiology, 2022, 29, 2694-2698.	2.1	4
48	(18)F-FDG PET/CT Imaging of Primary Hepatic Neuroendocrine Tumor. Asia Oceania Journal of Nuclear Medicine and Biology, 2015, 3, 58-60.	0.1	4
49	Temporal and spatial changes in reactive astrogliosis examined by 18F-THK5351 positron emission tomography in a patient with severe traumatic brain injury. European Journal of Hybrid Imaging, 2021, 5, 26.	1.5	4
50	Dual time point FDG PET for evaluation of malignant pleural mesothelioma. Nuclear Medicine Communications, 2009, 30, 25-9.	1.1	4
51	Fully parametric imaging with reversible tracer 18F-FLT within a reasonable time. Radiological Physics and Technology, 2017, 10, 41-48.	1.9	3
52	Multiple positron emission tomography tracers for use in the classification of gliomas according to the 2016 World Health Organization criteria. Neuro-Oncology Advances, 2021, 3, vdaa172.	0.7	3
53	Fractal analysis of 11C-methionine PET in patients with newly diagnosed glioma. EJNMMI Physics, 2021, 8, 76.	2.7	3
54	A Case of Ewing Sarcoma of the Mandible on F-FDG PET/CT. Asia Oceania Journal of Nuclear Medicine and Biology, 2020, 8, 84-87.	0.1	3

Υυκα Υαμαμότο

#	Article	IF	CITATIONS
55	The effect of zoledronic acid and denosumab on the mandible and other bones: a 18F-NaF-PET study. Oral Radiology, 2022, 38, 594-600.	1.9	3
56	Distinguishing between primary central nervous system lymphoma and glioblastoma using [18F]fluoromisonidazole and [18F]FDG PET. Nuclear Medicine Communications, 2022, 43, 270-274.	1.1	3
57	Correlation of 4′-[methyl-11C]-thiothymidine uptake with human equilibrative nucleoside transporter-1 and thymidine kinase-1 expressions in patients with newly diagnosed gliomas. Annals of Nuclear Medicine, 2018, 32, 634-641.	2.2	2
58	Occasionally increased 18F-FDG uptake in apical hypertrophic cardiomyopathy on serial follow-up PET/CT. Journal of Nuclear Cardiology, 2019, 26, 2125-2128.	2.1	2
59	Interim 4′-[methyl-11C]-thiothymidine PET for predicting the chemoradiotherapeutic response in head and neck squamous cell carcinoma: comparison with [18F]FDG PET. EJNMMI Research, 2021, 11, 13.	2.5	2
60	Effect of quantitative values on shortened acquisition duration in brain tumor 11C-methionine PET/CT. EJNMMI Physics, 2021, 8, 34.	2.7	2
61	Texture indices of 4′-[methyl-11C]-thiothymidine uptake predict p16 status in patients with newly diagnosed oropharyngeal squamous cell carcinoma: comparison with 18F-FDG uptake. European Journal of Hybrid Imaging, 2020, 4, 20.	1.5	2
62	SPECT/CT imaging in bone scintigraphy of a case of clavicular osteoma. Asia Oceania Journal of Nuclear Medicine and Biology, 2014, 2, 73-4.	0.1	2
63	Texture Indices of 18F-FDG PET/CT for Differentiating Squamous Cell Carcinoma and Non-Hodgkin's Lymphoma of the Oropharynx. Acta Medica Okayama, 2021, 75, 351-356.	0.2	2
64	Radiosynthesis of 18F-labeled d-allose. Carbohydrate Research, 2019, 486, 107827.	2.3	1
65	AB0595â€THE USEFULNESS OF 18F-FLUORODEOXYGLUCOSE POSITRON EMISSION TOMOGRAPHY CT (18F-	FDG) Tj ET	<sup>-</sup> Qq] 1 0.7843
66	Early infected aneurysm with 18F-FDG uptake prior to substantial anatomical changes. Journal of Nuclear Cardiology, 2019, 26, 1373-1375.	2.1	1
67	A preliminary study of relationship among the degree of internal carotid artery stenosis, wall shear stress on MR angiography and 18F-FDG uptake on PET/CT. Journal of Nuclear Cardiology, 2022, 29, 569-577.	2.1	1
68	Focal myocardial perfusion abnormalities in cardiac amyloidosis as compared with CMR, bone scintigraphy, and 11C-PiB PET. Journal of Nuclear Cardiology, 2021, 28, 2408-2411.	2.1	1
69	Left ventricular thrombus on 18F-FDG and 18F-FLT PET/CT in a patient with cardiac sarcoidosis. Journal of Nuclear Cardiology, 2021, 28, 2403-2407.	2.1	1
70	The potential relationship between 18F-FDG uptake and wall shear stress in a patient with carotid artery disease. Journal of Nuclear Cardiology, 2021, 28, 367-370.	2.1	1
71	Correlation of 4′-[methyl-11C]-thiothymidine PET with Gd-enhanced and FLAIR MRI in patients with newly diagnosed glioma. EJNMMI Research, 2021, 11, 42.	2.5	1
72	Whole-body PET angiography on semiconductor PET/CT. Journal of Nuclear Cardiology, 2022, 29, 885-888.	2.1	1

Υυκα Υαμαμότο

#	Article	IF	CITATIONS
73	Hypoxia and glucose metabolism assessed by FMISO and FDG PET for predicting IDH1 mutation and 1p/19q codeletion status in newly diagnosed malignant gliomas. EJNMMI Research, 2021, 11, 67.	2.5	1
74	Combination of whole body [18F]FDG PET angiography and PET/CT for giant cell arteritis. European Journal of Nuclear Medicine and Molecular Imaging, 2021, , 1.	6.4	1
75	Uptake protrusion on MPI indicating left ventricular diverticulum. Journal of Nuclear Cardiology, 2023, 30, 826-829.	2.1	1
76	Cardiac Sarcoidosis Mimicking Lymphoma in a Patient With Sjogren's Syndrome. Korean Circulation Journal, 2022, 52, 715.	1.9	1
77	The Studies of <i>in Vivo</i> Distributions of Radioiodinated Cobalt-bleomycin in Tumor-bearing Animals by the Whole Body Autoradiography. Radioisotopes, 2017, 66, 307-310.	0.2	Ο
78	Myocarditis with high 18F-FDG uptake and no 18F-FLT uptake. Journal of Nuclear Cardiology, 2018, 25, 691-692.	2.1	0
79	Radiation-induced myocardial damage indicated by focal defect on 123I-MIBG SPECT. European Journal of Nuclear Medicine and Molecular Imaging, 2019, 46, 2404-2405.	6.4	Ο
80	Non-ECG gated CT in a case of takotsubo cardiomyopathy. Journal of Cardiovascular Computed Tomography, 2020, 14, e46-e48.	1.3	0
81	Regional 18F-FDG uptake indicates coronary artery anomaly in a middle-aged patient with no atherosclerosis risk. Journal of Nuclear Cardiology, 2020, 27, 691-694.	2.1	Ο
82	Reverse redistribution on 201Tl SPECT in a patient with coronary artery ectasia. Journal of Nuclear Cardiology, 2022, 29, 857-860.	2.1	0
83	Cardiac sympathetic denervation in coronary artery fistula. Journal of Nuclear Cardiology, 2022, 29, 1457-1459.	2.1	0
84	Hypertrophic cardiomyopathy incidentally detected by 99mTc-HAS-D scintigraphy. Journal of Nuclear Cardiology, 2021, 28, 2374-2378.	2.1	0
85	99mTc-HSA-DTPA Scintigraphy of Protein-Losing Gastroenteropathy Associated with Mixed Connective Tissue Disease Before and After Immunosuppressive Therapy. Nuclear Medicine and Molecular Imaging, 2021, 55, 46-47.	1.0	Ο
86	Potential utility of 18F-NaF PET/CT in cardiac amyloidosis. Journal of Nuclear Cardiology, 2022, 29, 3557-3561.	2.1	0
87	Incidental 18F-FDG myocardial uptake revealed as physiological lesion by 18F-FLT PET/CT. Journal of Nuclear Cardiology, 2022, 29, 3579-3582.	2.1	0
88	Clinical significance of PET angiography in Takayasu arteritis. Journal of Nuclear Cardiology, 2022, 29, 3576-3578.	2.1	0
89	Abnormal FDG Biodistribution in a Patient With Gitelman Syndrome. Clinical Nuclear Medicine, 2021, 46, e264-e265.	1.3	0
90	What is this image? 2022 image 5 result. Journal of Nuclear Cardiology, 2022, 29, 403-408.	2.1	0

#	Article	IF	CITATIONS
91	LV functional evaluation on 11C-PiB PET/CT in cardiac amyloidosis. Journal of Nuclear Cardiology, 2023, 30, 1693-1696.	2.1	0